Letter

Even-odd effect on robustness of Majorana edge states in short Kitaev chains

Motohiko Ezawa
Department of Applied Physics, University of Tokyo, Hongo 7-3-1, Tokyo 113-8656, Japan

(Received 12 November 2023; accepted 3 April 2024; published 22 April 2024)

We construct two-band effective models describing Majorana edge states in a short Kitaev chain. We derive an analytical formula for the effective Hamiltonian as a function of model parameters. Then, we discuss the robustness of Majorana edge states as a function of model parameters. We have found an even-odd effect on the robustness of Majorana states, which is characteristic of short Kitaev chains. It is experimentally observable as a differential conductance in quantum dot systems. We also study effects of coupling to an environment based on non-Hermitian Hamiltonians derived from the Lindblad equation. It is found that the Majorana zero-energy edge states acquire nonzero energy such as $E \propto \pm(i\Gamma)^L$ for the local dissipation, where Γ is the magnitude of the dissipation and L is the length of the chain. The even-odd effect is manifest for small L in this formula. On the other hand, the Majorana zero-energy edge states acquire nonzero energy such as $E \propto \pm i\Gamma$ for small Γ irrespective of the length L for the global dissipation.

DOI: 10.1103/PhysRevB.109.L161404

Introduction. Majorana fermions are basic ingredients of topological quantum computation [1–6]. The Majorana edge states form a nonlocal qubit, which is robust against local perturbation due to topological protection. Thus, the qubit based on Majorana fermions will resolve the problem of decoherence in quantum computation. Majorana fermions must be materialized in topological superconductors [7–10], although their experimental realization is still controversial. The simplest model of a topological superconductor hosting Majorana fermions is the Kitaev chain [11]. Despite the simplicity of the model, it is hard to materialize it because it is hard to realize the p-wave superconducting order on the lattice. Although there are several proposals on the detection of the signature of Majorana fermions including fractional quantum Hall effects and Kitaev spin liquids, no compelling evidence of Majorana fermions has been obtained.

According to recent reports [12,13], the two-site and three-site Kitaev chains were experimentally realized in quantum dots. They evoke studies on the minimal Kitaev chain based on double quantum dots [14–21] and a few quantum dots [22–24]. For future topological quantum computation, it is desirable to materialize Majorana states with a minimal component, where the short Kitaev chain is an ideal platform. However, the Majorana edge states in a short Kitaev chain are not topologically protected. Indeed, we need a precise tuning of the model parameters so that the Majorana edge states exist exactly at the zero energy. There are studies on the condition for the Majorana edge states to have exact zero energy [25–29]. It is intriguing to estimate the robustness of the Majorana edge states for a short Kitaev chain. It is discussed [11] that the robustness of the Majorana zero-energy states increases exponentially as a function of the length of the Kitaev chain. Eventually, if the length of the Kitaev chain is long enough, the Majorana edge states are topological protected.

The platform of the Majorana fermions such as a quantum dot system has an interaction with another system such as a substrate. In general, the coupling to the bath makes the system an open quantum system. It is commonly analyzed based on the Lindblad equation [30]. The short-time dynamics is well described by a non-Hermitian Hamiltonian derived from the Lindblad equation [30]. A Kitaev chain with loss and gain has been studied in the context of a non-Hermitian Hamiltonian for a sufficiently long chain [31–44]. A Kitaev chain interacting with its environment has also been studied for a sufficiently long chain [45–47].

In this paper, we investigate numerically and analytically the robustness of the Majorana edge states in a short Kitaev chain. We construct an effective two-band model by using the isospectral matrix reduction method [48,49]. First, we study the Hamiltonian in the absence of dissipation. We have found an even-odd effect on the robustness of Majorana states as a function of the length L of the Kitaev chain, which is characteristic of short chains. It is possible to observe this phenomenon by measuring the differential conductance in quantum dot systems. Next, we study the Hamiltonian in the presence of local dissipation. We show that the Majorana edge states have energy $E \propto \pm(i\Gamma)^L$, where the even-odd effect with respect to L is manifest.

Kitaev chain. The Kitaev p-wave superconductor model is defined on the 1D lattice as [8,11]

$$\hat{H} = -\mu\sum_{x=1}^{L} c_x^\dagger c_x - t\sum_{x=1}^{L-1}(c_x^\dagger c_{x+1} + c_{x+1}^\dagger c_x) - \sum_{x=1}^{L-1}(\Delta c_x c_{x+1} + \Delta c_{x+1}^\dagger c_x^\dagger), \tag{1}$$

where μ is the chemical potential, $t > 0$ is the nearest-neighbor hopping strength, Δ is the p-wave pairing amplitude of the superconductor, and L is the length of the chain. An illustration of the Kitaev chain is shown in Fig. 1.

This model hosts two Majorana zero-energy edge states at both ends of a finite chain for $|\mu| < 2t$. The energy

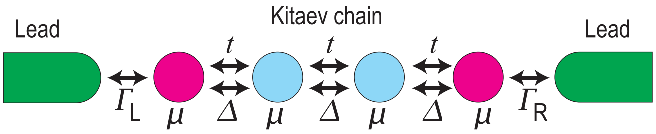

FIG. 1. Illustration of the Kitaev model with length $L = 4$ coupled with two leads, where μ is the chemical potential, $t > 0$ is the nearest-neighbor hopping strength, and Δ is the p-wave pairing amplitude of the superconductor. Magenta disks indicate the Majorana edge states. Γ_L (Γ_R) is a coupling between the left (right) quantum dot and the left (right) lead.

spectrum is exactly solvable at $|\Delta| = t$ and $\mu = 0$, where the penetration length is exactly zero. See Sec. I of the Supplemental Material [52] on this point. Hence, the Majorana edge states emerge even in the two-site system at these parameters.

We show the energy spectrum of Eq. (1) as a function of Δ/t for $L = 2, 3, 4, 5, 6$ in Figs. 2(a1)–2(a5) and that as a function of μ/t in Figs. 2(b1)–2(b5). Especially, the energy has a linear dependence $E = |\Delta - t|$ for the two-site Kitaev chain with $\mu = 0$ as shown in Fig. 2(a1). On the other hand, the energy has a parabolic dependence $E \propto \mu^2/t$ for the two-site Kitaev chain with $\Delta = t$ as shown in Fig. 2(b1).

The real part of the energy is exactly zero for the model with odd L as shown in Figs. 2(a2) and 2(a4). We will analytically verify these results by deriving an effective two-band model in the following.

The energy of free Majorana fermions should be exactly zero in topological superconductors. However, it acquires a nonzero real energy for a finite length chain as in Fig. 2 in general, because there is an overlap between the left and right edge states. There is an exceptional case of $|\Delta| = t$ and $\mu = 0$, where the penetration length of the Majorana edge state is exactly zero irrespective of the value L, as we review in Sec. I of the Supplemental Material [52]. Since the energy is exactly zero, the Majorana states are robust in this exceptional case. We note that the robustness is estimated by the amount of how much their energy is different from zero.

Effective two-band model. In order to reveal the behavior of the energy of Majorana states analytically near the exactly solvable point with the parameters $|\Delta| = t$ and $\mu = 0$, we construct an effective two-band model based on the isospectral matrix reduction method [48,49]. As we give a detailed derivation in Sec. II of the Supplemental Material [52],

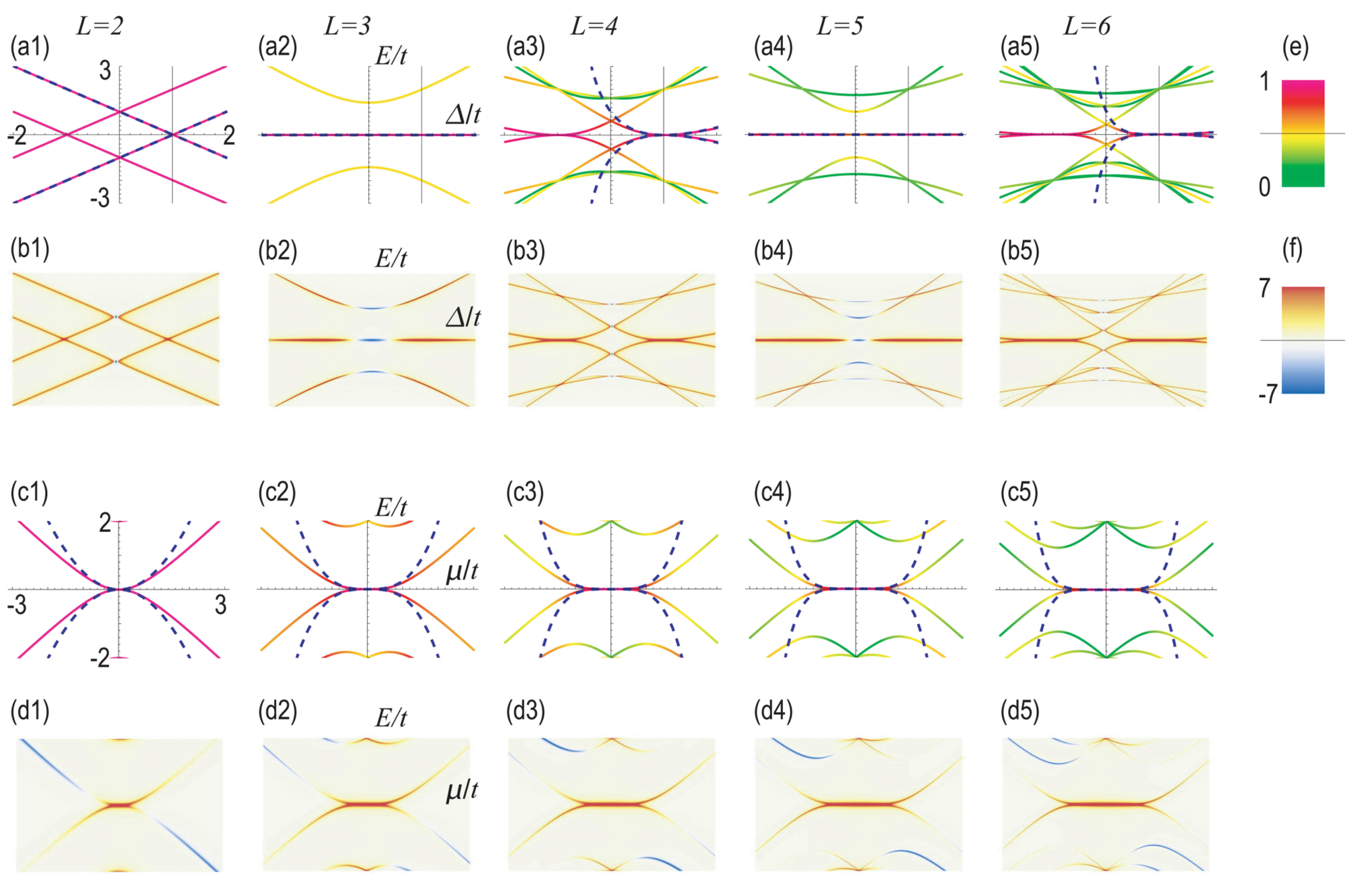

FIG. 2. (a1)–(a5) Energy E/t as a function of Δ/t. (b1)–(b5) Differential conductance in the Δ/t-E/t plane. We have set $\mu = 0$. (c1)–(c5) The energy E/t as a function of μ/t. (d1)–(d5) Differential conductance in the μ/t-E/t plane. We have set $\Delta = t$. (a1)–(d1) $L = 2$, (a2)–(d2) $L = 3$, (a3)–(d3) $L = 4$, (a4)–(d4) $L = 5$, and (a5)–(d5) $L = 6$. Blue dotted curves are the energy derived from the effective two-band model. (e) Color palette for (a1)–(a5) and (c1)–(c5) indicating the amplitude at the edge sites, where red color indicates the edge states and the green color indicates the bulk states. (f) Color palette for (b1)–(b5) and (d1)–(d5) indicating the magnitude of the differential conductance. We have set $\Gamma_L = \Gamma_R = 0.1t$.

we obtain

$$H_{\text{eff}} = \frac{(-1)^{L+1}}{(\Delta + t)^{L-1}} \sum_{m=0}^{\lfloor L/2 \rfloor} \binom{L-m}{m} \mu^{L-2m} (\Delta^2 - t^2)^m \sigma_y \quad (2)$$

for $L \geqslant 2$, where $\binom{L-m}{m}$ is a binomial coefficient.

If $\mu = 0$ in (2), we have $H_{\text{eff}} = 0$ for odd L, which well describes the energy near the zero energy as shown in Figs. 2(a2) and 2(a4). On the other hand, we have

$$H_{\text{eff}} = -\frac{(\Delta - t)^{L/2}}{(\Delta + t)^{L/2-1}} \sigma_y \quad (3)$$

for even L, which well describes the energy near the zero energy as shown in Figs. 2(a1), 2(a3), and 2(a5). The energy spectrum in the vicinity of the zero energy is significantly different between even and odd length of the chain. This is the even-odd effect, which is negligible for longer chains. According to Eq. (3) the energy is almost zero for small $|\Delta - t|$ and large L, implying that the Majorana edge states are robust.

If $\Delta = t$ in (2), we have

$$H_{\text{eff}} = -\frac{\mu^L}{(2t)^{L-1}} \sigma_y. \quad (4)$$

It fits well the energy near the zero energy as shown in Figs. 2(b1)–2(b5). It is almost zero for small μ and large L, implying that the Majorana edge states are robust.

Differential conductance. Differential conductance is an experimentally measurable quantity in quantum dot systems [12,13]. It is calculated based on the S-matrix theory in the wideband limit [12,50]. The S matrix is calculated as

$$S(E) = \begin{pmatrix} S_{\text{ee}}(E) & S_{\text{eh}}(E) \\ S_{\text{he}}(E) & S_{\text{hh}}(E) \end{pmatrix} = 1 - iW^\dagger \left(E - H + \frac{i}{2} W W^\dagger \right)^{-1} W, \quad (5)$$

where

$$W \equiv \text{diag}\{\sqrt{\Gamma_{\text{L}}}, 0, \ldots, 0, \sqrt{\Gamma_{\text{R}}}, -\sqrt{\Gamma_{\text{L}}}, 0, \ldots, 0, -\sqrt{\Gamma_{\text{R}}}\} \quad (6)$$

is the tunnel matrix, with Γ_α being the tunnel coupling strength between the dot α and the lead α ($\alpha = \text{L, R}$). See Fig. 1. The zero-temperature differential conductance is obtained as [12,50]

$$G_{\alpha\beta}(E) = \frac{dI_\alpha}{dV_\beta} = \frac{e^2}{h} \left(\delta_{\alpha\beta} - \left| S_{\text{ee}}^{\alpha\beta}(E) \right|^2 + \left| S_{\text{he}}^{\alpha\beta}(E) \right|^2 \right). \quad (7)$$

We show the differential conductance G_{LL} as a function of Δ/t and E/t in Figs. 2(b1)–2(b5) and that as a function of μ/t and E/t in Figs. 2(d1)–2(d5). They well agree with the energy spectra shown in Figs. 2(a1)–2(a5) and Figs. 2(c1)–2(c5), respectively. Hence, the energy spectrum is experimentally observable in quantum dots.

Open quantum system. The effects of the coupling between the system and an environment are described by the Lindblad equation [30] for the density matrix ρ as

$$\frac{d\rho}{dt} = -\frac{i}{\hbar}[\hat{H}, \rho] + \left(\sum_\alpha L_\alpha \rho L_\alpha^\dagger - \frac{1}{2}\{L_\alpha^\dagger L_\alpha, \rho\} \right), \quad (8)$$

where $\hat{H}$ is given by Eq. (1) and L is the Lindblad operator describing the dissipation.

This equation is rewritten in the form of

$$\frac{d\rho}{dt} = -\frac{i}{\hbar}(\hat{H}_{\text{total}}\rho - \rho \hat{H}_{\text{total}}^\dagger) + \sum_\alpha L_\alpha \rho L_\alpha^\dagger, \quad (9)$$

where $\hat{H}_{\text{total}}$ is a non-Hermitian effective Hamiltonian defined by $\hat{H}_{\text{total}} \equiv \hat{H} + \hat{H}_{\text{dissipation}}$ with the dissipation Hamiltonian

$$\hat{H}_{\text{dissipation}} \equiv -\frac{i\hbar}{2} \sum_\alpha L_\alpha^\dagger L_\alpha. \quad (10)$$

It describes a short-time dynamics [30]. We show the derivation of Eqs. (9) and (10) in Sec. III of the Supplemental Material [52].

Local dissipation. We study the local dissipation [42,51], where the Lindblad operators are given by

$$L_x^- = \sqrt{\Gamma_-} c_x, \quad L_x^+ = \sqrt{\Gamma_+} c_x^\dagger, \quad (11)$$

where $\Gamma_\pm$ represent the dissipation. They describe the effect that the particle is coming in and out of a single site. There is a relation [51]

$$\frac{\Gamma_- - \Gamma_+}{\Gamma_- + \Gamma_+} = \tanh \frac{\mu\beta}{2}, \quad (12)$$

where $\beta \equiv 1/k_{\text{B}}T$ is the inverse temperature. The corresponding dissipation Hamiltonian reads

$$\hat{H}_{\text{dissipation}} = -\frac{i\hbar}{2} \sum_{x=1}^{L} [\Gamma c_x^\dagger c_x + \Gamma_+], \quad (13)$$

where $\Gamma \equiv \Gamma_- - \Gamma_+$. We give a derivation of Eq. (13) in Sec. III of the Supplemental Material [52].

By introducing a complex chemical potential

$$\tilde{\mu} = \mu + \frac{i\hbar}{2}\Gamma, \quad (14)$$

the effect of the local dissipation is fully taken into account. We show the energy spectrum as a function of Γ in Fig. 3 by diagonalizing the Hamiltonian (1) together with (13), where we have omitted the constant term $-i\hbar L\Gamma_+/2$ in (13). The real part of the energy for odd length is exactly zero as shown in Figs. 3(a2) and 3(a4). On the other hand, the imaginary part of the energy for even length is exactly zero if the dissipation is smaller than a certain critical value $|\Gamma| < |\Gamma_{\text{critical}}|$.

The flat region of the zero-energy Majorana edge states expands for longer chains. These properties are explained based on the effective model with local dissipation. By inserting Eq. (14) into (2), we obtain

$$H_{\text{eff}} = -\frac{(i\hbar\Gamma/2)^L}{(2t)^{L-1}} \sigma_y \quad (15)$$

for $L \geqslant 2$, $\Delta = t$, and $\mu = 0$. This formula well explains the fact that the real [imaginary] part of the energy is zero for even [odd] L as depicted by blue dotted curves in Figs. 3(a2) and 3(a4) [Figs. 3(b1) and 3(b3)]. The even-odd effect is manifest also in the presence of the local dissipation. The Majorana edge state becomes robust for a long chain provided $|\hbar\Gamma/2t| < 1$.

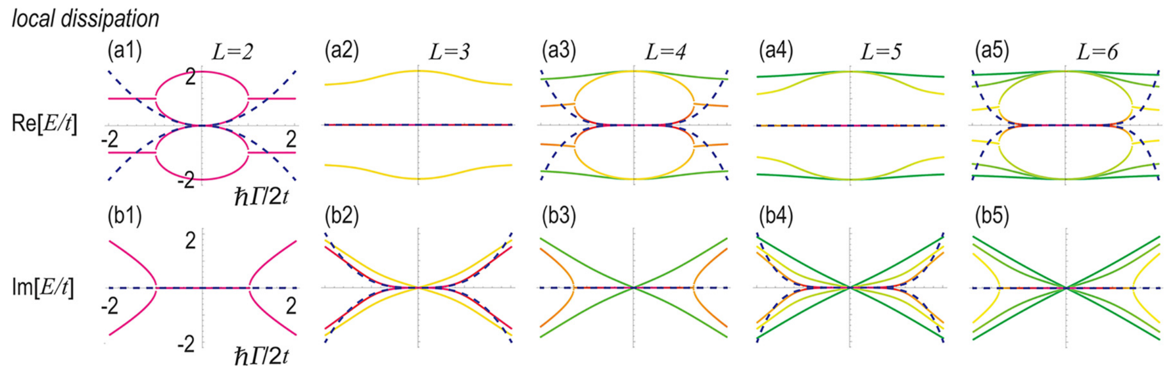

FIG. 3. (a1)–(a4) Real part and (b1)–(b4) imaginary part of the energy as a function of the local dissipation $\hbar\Gamma/2t$. (a1) and (b1) $L = 2$, (a2) and (b2) $L = 3$, (a3) and (b3) $L = 4$, (a4) and (b4) $L = 5$, (a5) and (b5) $L = 6$. We have set $\Delta = t$ and $\mu = 0$. Blue dotted curves are the energy derived from the effective two-band model. See the color palette in Fig. 2.

A comment is in order. The Majorana edge state acquires nonzero pure imaginary energy for odd L in Eq. (15). It means that the lifetime of the Majorana state becomes finite. Even in the presence of the non-Hermitian term, particle-hole symmetry is preserved and Majorana states are intact [39].

We can also study the adjacent and the global dissipation, whose results are shown in Secs. IV and V of the Supplemental Material [52], respectively. In particular, the Majorana zero-energy edge states acquire nonzero energy such as $E \propto \pm i\Gamma$ for small Γ irrespective of the length L for the global dissipation.

Discussion. We have proposed and analytically studied two-band effective models describing the Majorana edge states in a chain with length L, motivated by recent experiments on quantum dots. We have predicted the even-odd effect on the robustness of the Majorana states in short Kitaev chain. Especially, we have found that the Majorana states in the Kitaev chain with $L = 3$ is more robust than that with $L = 4$ as a function of Δ, which is an unexpected result. It will be observed in the system of quantum dot systems by measuring the differential conductance.

The status of experiments on quantum dots is still in the beginning stage. The four- and five-site Kitaev models will be realized based on four and five quantum dots soon. Our results provide a criterion of how much it is necessary to tune the parameters and dissipations to increase the robustness of Majorana states in a short Kitaev chain with various L. In addition, we can check whether the Kitaev model is actually realized in experiments by observing the behavior of the energy by way of intentionally tuning away from the exactly solvable parameters $\Delta = t$ and $\mu = 0$. They will be useful for future experimental works of the short Kitaev chain based on quantum dots.

Acknowledgments. This work is supported by CREST, JST (Grant No. JPMJCR20T2) and a Grant-in-Aid for Scientific Research from MEXT KAKENHI (Grant No. 23H00171).

[1] S. B. Bravyi and A. Y. Kitaev, Fermionic quantum computation, Ann. Phys. **298**, 210 (2002).
[2] D. A. Ivanov, Non-Abelian statistics of half-quantum vortices in p-wave superconductors, Phys. Rev. Lett. **86**, 268 (2001).
[3] A. Kitaev, Fault-tolerant quantum computation by anyons, Ann. Phys. **303**, 2 (2003).
[4] S. Das Sarma, M. Freedman, and C. Nayak, Topologically protected qubits from a possible non-Abelian fractional quantum Hall state, Phys. Rev. Lett. **94**, 205501 (2005).
[5] C. Nayak, S. H. Simon, A. Stern, M. Freedman, and S. Das Sarma, Non-Abelian anyons and topological quantum computation, Rev. Mod. Phys. **80**, 1083 (2008).
[6] M. Ezawa, Systematic construction of topological-nontopological hybrid universal quantum gates based on many-body Majorana fermion interactions, arXiv:2304.06260.
[7] X.-L. Qi and S.-C. Zhang, Topological insulators and superconductors, Rev. Mod. Phys. **83**, 1057 (2011).
[8] J. Alicea, New directions in the pursuit of Majorana fermions in solid state systems, Rep. Prog. Phys. **75**, 076501 (2012).
[9] M. Sato and Y. Ando, Topological superconductors: A review, Rep. Prog. Phys. **80**, 076501 (2017).
[10] J. Alicea, Y. Oreg, G. Refael, F. von Oppen, and M. P. A. Fisher, Non-Abelian statistics and topological quantum information processing in 1D wire networks, Nat. Phys. **7**, 412 (2011).
[11] A. Y. Kitaev, Unpaired Majorana fermions in quantum wires, Phys. Usp. **44**, 131 (2001).
[12] T. Dvir, G. Wang, N. van Loo, C.-X. Liu, G. P. Mazur, A. Bordin, S. L. D. Ten Haaf, J.-Y. Wang, D. V. Driel, F. Zatelli, X. Li, F. K. Malinowski, S. Gazibegovic, G. Badawy, E. P. A. M. Bakkers, M. Wimmer, and L. P. Kouwenhoven, Realization of a minimal Kitaev chain in coupled quantum dots, Nature (London) **614**, 445 (2023).
[13] A. Bordin, X. Li, D. V. Driel, J. C. Wolff, Q. Wang, S. L. D. ten Haaf, G. Wang, N. V. Loo, L. P. Kouwenhoven, and T. Dvir, Crossed Andreev reflection and elastic cotunneling in three quantum dots coupled by superconductors, Phys. Rev. Lett. **132**, 056602 (2024).
[14] A. Tsintzis, R. S. Souto, and M. Leijnse, Creating and detecting poor man's Majorana bound states in interacting quantum dots, Phys. Rev. B **106**, L201404 (2022).
[15] C.-X. Liu, G. Wang, T. Dvir, and M. Wimmer, Tunable superconducting coupling of quantum dots via Andreev bound states

in semiconductor-superconductor nanowires, Phys. Rev. Lett. **129**, 267701 (2022).

[16] C.-X. Liu, H. Pan, F. Setiawan, M. Wimmer, and J. D. Sau, Fusion protocol for Majorana modes in coupled quantum dots, Phys. Rev. B **108**, 085437 (2023).

[17] R. Koch, D. V. Driel, A. Bordin, J. L. Lado, and E. Greplova, Adversarial Hamiltonian learning of quantum dots in a minimal Kitaev chain, Phys. Rev. Appl. **20**, 044081 (2023).

[18] A. Tsintzis, R. S. Souto, K. Flensberg, J. Danon, and M. Leijnse, Majorana qubits and non-Abelian physics in quantum dot-based minimal Kitaev chains, PRX Quantum **5**, 010323 (2024).

[19] D. M. Pino, R. S. Souto, and R. Aguado, Minimal Kitaev-transmon qubit based on double quantum dots, Phys. Rev. B **109**, 075101 (2024).

[20] W. Samuelson, V. Svensson, and M. Leijnse, A minimal quantum dot-based Kitaev chain with only local superconducting proximity effect, Phys. Rev. B **109**, 035415 (2024).

[21] C.-X. Liu, A. M. Bozkurt, F. Zatelli, S. L. D. ten Haaf, T. Dvir, and M. Wimmer, Enhancing the excitation gap of a quantum-dot-based Kitaev chain, arXiv:2310.09106.

[22] M. Mohseni, H. Allami, D. Miravet, D. J. Gayowsky, M. Korkusinski, and P. Hawrylak, Majorana excitons in a Kitaev chain of semiconductor quantum dots in a nanowire, Nanomaterials **13**, 2293 (2023).

[23] R. S. Souto, A. Tsintzis, M. Leijnse, and J. Danon, Probing Majorana localization in minimal Kitaev chains through a quantum dot, Phys. Rev. Res. **5**, 043182 (2023).

[24] S. Miles, D. V. Driel, M. Wimmer, and C.-X. Liu, Kitaev chain in an alternating quantum dot–Andreev bound state array, arXiv:2309.15777.

[25] H.-C. Kao, Chiral zero modes in superconducting nanowires with Dresselhaus spin-orbit coupling, Phys. Rev. B **90**, 245435 (2014).

[26] S. Hegde, V. Shivamoggi, S. Vishveshwara, and D. Sen, Quench dynamics and parity blocking in Majorana wires, New J. Phys. **17**, 053036 (2015).

[27] A. A. Zvyagin, Majorana bound states in the finite-length chain, Low Temp. Phys. **41**, 625 (2015).

[28] C. Zeng, C. Moore, A. M. Rao, T. D. Stanescu, and S. Tewari, Analytical solution of the finite-length Kitaev chain coupled to a quantum dot, Phys. Rev. B **99**, 094523 (2019).

[29] N. Leumer, M. Marganska, B. Muralidharan, and M. Grifoni, Exact eigenvectors and eigenvalues of the finite Kitaev chain and its topological properties, J. Phys.: Condens. Matter **32**, 445502 (2020).

[30] G. Lindblad, On the generators of quantum dynamical semigroups, Commun. Math. Phys. **48**, 119 (1976).

[31] S. Diehl, E. Rico, M. A. Baranov, and P. Zoller, Topology by dissipation in atomic quantum wires, Nat. Phys. **7**, 971 (2011).

[32] X. Wang, T. Liu, and Y. Xiong, Spontaneous $\mathcal{PT}$-symmetry breaking in non-Hermitian Kitaev and extended Kitaev models, Phys. Rev. A **92**, 012116 (2015).

[33] C. Yuce, Majorana edge modes with gain and loss, Phys. Rev. A **93**, 062130 (2016).

[34] Q.-B. Zeng, B. Zhu, S. Chen, L. You, and R. Lu, Non-Hermitian Kitaev chain with complex on-site potentials, Phys. Rev. A **94**, 022119 (2016).

[35] K. Kawabata, Y. Ashida, H. Katsura, and M. Ueda, Parity-time-symmetric topological superconductor, Phys. Rev. B **98**, 085116 (2018).

[36] K. Kawabata, S. Higashikawa, Z. Gong, Y. Ashida, and M. Ueda, Topological unification of time-reversal and particle-hole symmetries in non-Hermitian physics, Nat. Commun. **10**, 297 (2019).

[37] K. Kawabata, K. Shiozaki, M. Ueda, and M. Sato, Symmetry and topology in non-Hermitian physics, Phys. Rev. X **9**, 041015 (2019).

[38] N. Shibata and H. Katsura, Dissipative spin chain as a non-Hermitian Kitaev ladder, Phys. Rev. B **99**, 174303 (2019).

[39] M. Ezawa, Braiding of Majorana-like corner states in electric circuits and its non-Hermitian generalization, Phys. Rev. B **100**, 045407 (2019).

[40] C. Zhang, L. Sheng, and D. Xing, Non-Hermitian disorder-driven topological transition in a dimerized Kitaev superconductor chain, Phys. Rev. B **103**, 224207 (2021).

[41] X.-M. Zhao, C.-X. Guo, S.-P. Kou, L. Zhuang, and W.-M. Liu, Defective Majorana zero modes in a non-Hermitian Kitaev chain, Phys. Rev. B **104**, 205131 (2021).

[42] S. Lieu, Non-Hermitian Majorana modes protect degenerate steady states, Phys. Rev. B **100**, 085110 (2019).

[43] A. Maiellaro and R. Citro, Non-Hermitian topological phases in an extended Kitaev model, J. Phys.: Conf. Ser. **1548**, 012026 (2020).

[44] S. Sayyad and J. L. Lado, Topological phase diagrams of exactly solvable non-Hermitian interacting Kitaev chains, Phys. Rev. Res. **5**, L022046 (2023).

[45] F. L. Pedrocchi and D. P. Di Vincenzo, Majorana braiding with thermal noise, Phys. Rev. Lett. **115**, 120402 (2015).

[46] F. L. Pedrocchi, N. E. Bonesteel, and D. P. Di Vincenzo, Monte Carlo studies of the self-correcting properties of the Majorana quantum error correction code under braiding, Phys. Rev. B **92**, 115441 (2015).

[47] Y. Hu, Z. Cai, M. A. Baranov, and P. Zoller, Majorana fermions in noisy Kitaev wires, Phys. Rev. B **92**, 165118 (2015).

[48] L. Eek, A. Moustaj, M. Rontgen, V. Pagneux, V. Achilleos, and C. M. Smith, Emergent non-Hermitian models, Phys. Rev. B **109**, 045122 (2024).

[49] M. Rontgen, X. Chen, W. Gao, M. Pyzh, P. Schmelcher, V. Pagneux, V. Achilleos, and A. Coutant, Latent Su-Schrieffer-Heeger models, arXiv:2310.07619.

[50] S. Datta, *Electronic Transport in Mesoscopic Systems* (Cambridge University Press, Cambridge, 1995); *Quantum Transport: Atom to Transistor* (Cambridge University Press, Cambridge, 2005).

[51] P. Kos and T. Prosen, Time-dependent correlation functions in open quadratic fermionic systems, J. Stat. Mech. (2017) 123103.

[52] See Supplemental Material at http://link.aps.org/supplemental/10.1103/PhysRevB.109.L161404 for the exact solvable condition in Sec. I, the isospectral matrix reduction method in Sec. II, the derivation of the effective model in Sec. III, the Lindblad equation in Sec. IV, effects of adjacent dissipation in Sec. V, effects of global dissipation in Sec. VI, and the minimal Kitaev chain in Sec. VII.